Square-Root Nyquist Filter Design for QAM-Based Filter Bank Multicarrier Systems

Sohail Taheri, Mir Ghoraishi, Pei Xiao, Lei Zhang, and Yu Xin

***Abstract*—Filter bank multicarrier systems with quadrature amplitude modulation (FBMC/QAM) have drawn attentions to get the advantage of complex symbol transmission, as well as very low out of band radiation and relaxed synchronization requirements for asynchronous scenarios. In order to make this system viable for practical deployment, the biggest challenge is designing appropriate filters to minimize the interference between adjacent subcarriers, while maintaining the Nyquist property of the filter. We show that the deviation from the Nyquist property can be compensated through the fractional shift of the filtered symbols, which provides flexibility to optimize the stopband of the filter. The proposed design method shows advantages over the state of the art designs, and provides guidance for the filter design in practical FBMC/QAM systems.**

I. Introduction

Several waveforms have been introduced as a potential replacement for orthogonal frequency division multiplexing (OFDM) to facilitate asynchronous transmissions and efficient use of available spectrum in the next generation of cellular systems. Filter bank multicarrier with offset quadrature amplitude modulation (FBMC/OQAM) is one of the promising candidates which provide very low out of band radiation (OoBR), as well as immunity against synchronization errors, thanks to its per-subcarrier filtering [1], [2].

The main drawback in FBMC/OQAM is that it relaxes the orthogonality condition to *real* field to utilize a well-localized filter in time and frequency, and maintain transmission at the Nyquist rate [3]. Consequently, the transmitted real symbols are contaminated with imaginary interference terms (intrinsic interference) when receiving the symbols. The interference terms are the main issue in the channel estimation process [3], [4] and multiple-input-multiple-output (MIMO) applications with the maximum likelihood detection [5] and the Alamouti space-time block coding [6].

The idea of FBMC with QAM modulation (FBMC/QAM) is reaching a quasi-orthogonal signal while maintaining per-subcarrier filtering. There are two approaches of FBMC/QAM in the literature. The first one, which is called Type I in this paper, was introduced in [7], [8] and uses two different prototype filters for odd and even subcarriers to mitigate intrinsic interference. One of the proposed filters in [7] suffers from very poor OoBR which was enhanced in [9] and [10]. Type II of FBMC/QAM introduced in [11] uses an optimized prototype filter for all subcarriers. Iterative receivers and an optimized filter aiming for reducing the residual intrinsic interference of this system were proposed in [12] and [9], respectively. The advantage of Type II is that the OoBR rapidly decays to the desired level within one subcarrier spacing. This type is also known as filter bank based OFDM (FB-OFDM) in [13]. However, the filter design in this approach is quite critical to achieving an acceptable level of orthogonality, while the filter keeps its Nyquist property in time domain.

In this paper, we target at filter design for type II of FBMC/QAM systems. The proposed filters in [9] and [13] suffer from relatively high level of interference in time domain and frequency domain, respectively. Therefore in this paper, we optimize the stopband of the prototype filter to reduce inter-carrier interference (ICI) between adjacent subcarriers. Moreover, we show that when the designed filter does not satisfy the Nyquist property, the resulting inter-symbol interference (ISI) error of the filter can be compensated through fractional shift of the filtered symbols. As a result, we can optimize the design to reduce the energy of intrinsic interference and reach a quasi-orthogonal system. Additionally, the result can be used in Type I systems as a primary filter, which eases the design of the secondary filter due to less interfering samples in frequency domain. The design process is inspired by a method proposed for single-carrier systems in [14]. This technique provides flexibility to control different parameters such as stopband attenuation, Nyquist property, and tails energy. However, the iterative optimization method proposed in [14] is not converging to the global minimum in some scenarios. Thus, we also derive an optimization method based on Newton-Raphson iterations to address the nonlinear problem solving in the filter design procedure.

The rest of this paper is organized as follows. In Sec II, the system model of FBMC/QAM is introduced, the interference terms when receiving the symbols are extracted, and the Nyquist property is discussed. In Sec. III, the filter design procedure is proposed and optimization targets are explained. Simulation results and performance of the system with comparison to the state of the art filters are provided in Sec. IV. Finally, the conclusions are drawn in Sec. V.

Notations: $\mathbb{R}$ and $\mathbb{C}$ are the field for real and complex numbers. $\mathbf{0}$, $\mathbf{0}_{a\times b}$, $\mathbf{I}_a$ are zero vector, $a \times b$ zero matrix, and $a \times a$ identity matrix, respectively. $[\mathbf{a}]_n$ is the nth element of the vector $\mathbf{a}$. $[\mathbf{A}]_{i,j}$ is the matrix element on ith row and jth column. $[\mathbf{A};\mathbf{B}]$ is vertical matrix concatenation. $\|\mathbf{a}\|$, $\mathbf{A}^{\mathrm{T}}$, and $\mathbf{A}^{\mathrm{H}}$ are vector norm, transpose, and Hermitian. $\delta_{a,b}$ is

Sohail Taheri and Pei Xiao are with the Institute for Communication Systems, University of Surrey, Guildford, GU2 7XH, UK. (email: {s.taheri, p.xiao}@surrey.ac.uk)

Mir Ghoraishi is with pureLiFi, 9 Haymarket Terrace, Edinburgh, UK, EH12 5EZ. (email: mir.ghoraishi@purelifi.com)

Lei Zhang is with the School of Engineering, University of Glasgow, Glasgow, UK, G12 8QQ. (email: lei.zhang@glasgow.ac.uk)

Yu Xin is with ZTE corporation, Shenzhen, P.R.China (email: xin.yu@zte.com.cn)

Kronecker delta function. $*$ and $\otimes$ are linear convolution and Kronecker product.

II. System Model

The general form of transmit signal for FBMC systems is

$$s[k] = \sum_{n=0}^{N-1} \sum_{m=0}^{M-1} a_{m,n} e^{j\frac{2\pi}{M}mk} g[k - nM], \tag{1}$$

where $a_{m,n}$ are the complex symbols with $m = 0, 1, \ldots, M-1$ and $n = 0, 1, \ldots, N-1$ as subcarrier index and symbol index respectively. $g[k]$ is a real-valued low-pass filter with the length $L_g = KM$. K is an integer number which indicates the overlap factor of the filter in frequency domain. The matrix representation of (1) can be written as

$$\mathbf{s} = \sum_{n=0}^{N-1} \mathbf{E}_n \mathbf{W}_{KM}^{\mathrm{H}} \bar{\mathbf{G}} \mathbf{a}_n, \tag{2}$$

where $\mathbf{a}_n \in \mathbb{C}^{M\times 1}$ is the symbol vector and and $\mathbf{W}_{KM}$ is a KM-sized FFT matrix. $\bar{\mathbf{G}} = [\mathbf{G}_0, \mathbf{G}_1, \ldots, \mathbf{G}_{M-1}] \in \mathbb{C}^{KM\times M}$ is the filter matrix in frequency domain, wherein $\mathbf{G}_0 = [G(0), G(1), \ldots, G(K-1), \mathbf{0}, G(-K+1), \ldots, G(-1)]^{\mathrm{T}} \in \mathbb{C}^{KM\times 1}$ is the FFT output of $\mathbf{g}$ (vector form of $g[k]$) and $\mathbf{G}_m$ are the cyclic shifts of $\mathbf{G}_0$ with mK units. Finally, $\mathbf{E}_n \in \mathbb{R}^{(N+K-1)M\times KM}$ is a shift matrix defined as

$$\mathbf{E}_n = [\mathbf{0}_{nM\times KM}; \mathbf{I}_{KM}; \mathbf{0}_{(N-n-1)M\times KM}], \tag{3}$$

which provides overlap-add operation. Assuming an ideal channel, i.e., no added noise and channel distortion, the demodulated symbols at the receiver side can be expressed as

$$\begin{aligned} \hat{\mathbf{a}}_n &= \bar{\mathbf{G}}^{\mathrm{T}} \mathbf{W}_{KM} \mathbf{E}_n^{\mathrm{T}} \mathbf{s} \\ &= \bar{\mathbf{G}}^{\mathrm{T}} \mathbf{W}_{KM} \mathbf{E}_n^{\mathrm{T}} \sum_{\bar{n}=-\infty}^{+\infty} \mathbf{E}_{\bar{n}} \mathbf{W}_{KM}^{\mathrm{H}} \bar{\mathbf{G}} \mathbf{a}_{\bar{n}} \\ &= \bar{\mathbf{G}}^{\mathrm{T}} \bar{\mathbf{G}} \mathbf{a}_n + \underbrace{\bar{\mathbf{G}}^{\mathrm{T}} \mathbf{W}_{KM} \mathbf{E}_n^{\mathrm{T}} \sum_{\bar{n}\neq n} \mathbf{E}_{\bar{n}} \mathbf{W}_{KM}^{\mathrm{H}} \bar{\mathbf{G}} \mathbf{a}_{\bar{n}}}_{\mathbf{a}_n^{\mathrm{ISI}}}. \end{aligned} \tag{4}$$

By defining $\bar{\mathbf{G}}^T \bar{\mathbf{G}} = \mathbf{I} + \mathbf{G}^{\mathrm{ICI}}$, (4) can be rephrased as

$$\begin{aligned} \hat{\mathbf{a}}_n &= \mathbf{a}_n + \mathbf{G}^{\mathrm{ICI}} \mathbf{a}_n + \mathbf{a}_n^{\mathrm{ISI}} \\ &= \mathbf{a}_n + \mathbf{a}_n^{\mathrm{ICI}} + \mathbf{a}_n^{\mathrm{ISI}}. \end{aligned} \tag{5}$$

As can be seen, $\mathbf{a}_n^{\mathrm{ICI}}$ and $\mathbf{a}_n^{\mathrm{ISI}}$ appear as intrinsic interference due to ICI and ISI at the receiver. The energy of these terms depend on the designed prototype filter $\mathbf{g}$. For conventional FBMC filters, the energy of ICI is significant [11]. In order to a have proper symbol detection, it is necessary to reduce the energy level of the ICI term.

Nyquist Property of The Prototype Filter

According to the Nyquist criterion for multicarrier systems, the matched filter which is the correlation of the transmit and receive prototype filters, i.e. $p[k] = g[k] * g[-k]$ should provide the following property

$$p[k] \sum_{n=-\infty}^{+\infty} \delta_{k,nM} = \delta_{k,0}. \tag{6}$$

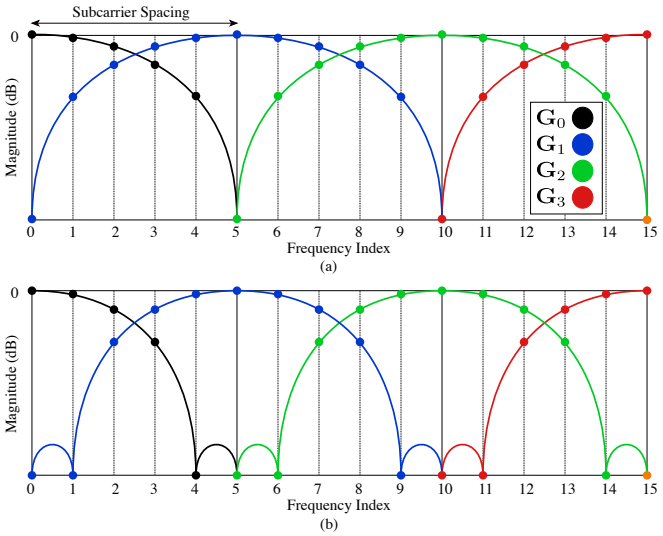

Fig. 1. Frequency domain representation of FBMC subcarriers in a limited range assuming $K = 5$. Dashed lines show the FFT sampling points. a) Conventional design for FBMC/OQAM, the adjacent subcarriers are overlapping on 4 non-zero samples. b) Target design for FBMC/QAM with reduced ICI energy, i.e. the number of non-zero overlapping samples is reduced to 2.

In multicarrier systems, if the matched filter does not strictly follow the Nyquist property, it is possible to choose a proper integer parameter ΔM to minimize $\mathbf{a}_n^{\mathrm{ISI}}$. The amount of ΔM is chosen according to zero-crossings of the matched filter in time domain. To this end, $\mathbf{E}_n$ in (3) is modified to

$$\mathbf{E}_n = [\mathbf{0}_{n(M+\Delta M)\times KM}; \mathbf{I}_{KM}; \mathbf{0}_{(N-n-1)(M+\Delta M)\times KM}]. \tag{7}$$

In this case, the spectral efficiency indicator (SEI) of the system, normalized to bit per symbol and coding rate, is defined as $\epsilon = M/(M + \Delta M)$. Although this fractional shift in overlap-add process leads to reduction of SEI, it enables the flexibility to optimize the stopband of the prototype filter, so that the energy of $\mathbf{a}_n^{\mathrm{ICI}}$ is minimized.

III. Filter Design Process

In this section, we provide a filter design method to obtain a prototype filter with reduced ICI energy. As mentioned earlier, $\mathbf{G}_0$ is the FFT output of the prototype filter $\mathbf{g}$ with length KM. Thus, $\mathbf{G}_0$ are the samples of the frequency response of $\mathbf{g}$ at $\Delta f = 1/(KM)$. In typical FBMC filters, where they are localized within one subcarrier spacing, the adjacent subcarriers have K samples overlap in frequency domain, and $\mathbf{G}_0$ will have only $2K-1$ non-zero samples. As shown in Fig. 1.(a), $K-1$ samples out of K overlapping samples are non-zero and contribute to ICI energy. Accordingly, reducing the non-zero overlapping samples leads to ICI energy reduction.

The design procedure of $\mathbf{g}$, to fulfill the condition mentioned above is enumerated as follows:

1) A single-carrier filter is defined in frequency domain as $\mathbf{G}_{\mathrm{s}} = [G(0), G(1), \ldots, G(K-1), 0, G(-K+1), \ldots, G(-1)]^{\mathrm{T}} \in \mathbb{R}^{2K\times 1}$, which contains the sequence of non-zero taps of $\mathbf{G}_0$.

$$\mathbf{g}_{\text{ls}}^{k+1} = \mathbf{g}_{\text{ls}}^{k} + \Big((\mathbf{A}'^{\text{T}}\mathbf{\Gamma}^2\mathbf{A}' + 2\sum_{n=0}^{L_{g_\text{s}}-1}[\mathbf{\Gamma}]_{n,n}\bar{\mathbf{S}}_n([\mathbf{\Gamma}\mathbf{A}\mathbf{g}_{\text{ls}}^{k}]_n - [\mathbf{\Gamma}\mathbf{u}]_n)\Big)^{-1}\mathbf{A}'^{\text{T}}\mathbf{\Gamma}^2(\mathbf{u} - \mathbf{A}\mathbf{g}_{\text{ls}}^{k}). \tag{20}$$

2) The time domain filter taps can be obtained as $\mathbf{g}_\text{s} = \text{IFFT}\{\mathbf{G}_\text{s}\}$. The target is to optimize $\mathbf{g}_\text{s}$ so that $G(K-1) = G(-K+1) \approx 0$, as shown in Fig. 1.(b).
3) The resulting $\mathbf{G}_\text{s}$ is zero-padded to reach the size KM and form $\mathbf{G}_0$.
4) The prototype filter $\mathbf{g}$ is extracted as $\mathbf{g} = \text{IFFT}\{\mathbf{G}_0\}$.

A. Single-carrier Design

The single-carrier filter design is based on two optimization goal which is described in the following.

The first optimization goal is to minimize the stopband of the filter. Defining z-transform of $\mathbf{g}_\text{s}$ as

$$G_\text{s}(z) = \sum_{n=0}^{L_{g_\text{s}}}[\mathbf{g}_\text{s}]_n z^{-n} = \mathbf{e}(z)\mathbf{g}_\text{s}, \tag{8}$$

wherein $\mathbf{e}(z) = [1, z^{-1}, \ldots, z^{-L_{g_\text{s}}}]$ and L_{g_s} is the length of $\mathbf{g}_\text{s}$, and assuming normalized frequency spectrum, the stopband energy of $\mathbf{g}_\text{s}$ is defined as

$$\xi_\text{s} = \int_{f_0}^{1-f_0} |G_s(e^{j2\pi f})|^2 df, \tag{9}$$

where f_0 is the stop frequency defined as $f_0 = (1+\alpha)/4$, and α is the roll-off factor of the filter. With some manipulations and using Parseval's theorem, it is easy to show that [14]

$$\xi_\text{s} = \mathbf{g}_\text{s}^\text{T}\mathbf{\Phi}\mathbf{g}_\text{s}, \tag{10}$$

where,

$$[\mathbf{\Phi}]_{i,j} = \begin{cases} 1 - 2f_0, & i = j \\ -2f_0\text{sinc}\big(2f_0(i-j)\big). & i \neq j \end{cases} \tag{11}$$

We assume that $\mathbf{g}_\text{s}$ is symmetric odd length (FIR Type I). In this case, to reduce the computation complexity, it is possible to exploit only half of the filter $\mathbf{g}_\text{s}$ in the calculations. Thus, we can define $\mathbf{g}_{\text{ls}} = [g_s[0], \ldots, g_s[(L_{g_\text{s}}-1)/2]^\text{T} \in \mathbb{R}^{L_{g_\text{ls}}\times 1}$ as the left half of $\mathbf{g}_\text{s}$, where $L_{g_\text{ls}} = (L_{g_\text{s}}+1)/2$. Also, a mapping matrix $\mathbf{O} \in \mathbb{R}^{L_{g_\text{s}}\times L_{g_\text{ls}}}$ is defined to construct $\mathbf{g}_\text{s}$ from $\mathbf{g}_\text{ls}$, so that $\mathbf{g}_\text{s} = \mathbf{O}\mathbf{g}_\text{ls}$. In this case, (10) can be rewritten as

$$\xi_\text{s} = \mathbf{g}_\text{ls}^\text{T}\mathbf{O}^\text{T}\mathbf{\Phi}\mathbf{O}\mathbf{g}_\text{ls} = \mathbf{g}_\text{ls}^\text{T}\bar{\mathbf{\Phi}}\mathbf{g}_\text{ls} = \mathbf{g}_\text{ls}^\text{T}\mathbf{\Lambda}^\text{T}\mathbf{\Lambda}\mathbf{g}_\text{ls} = \|\mathbf{\Lambda}\mathbf{g}_\text{ls}\|^2. \tag{12}$$

in (12), $\bar{\mathbf{\Phi}} = \mathbf{\Lambda}^\text{T}\mathbf{\Lambda}$ is the Cholesky factorization.

To minimize the stopband ξ_s, the first optimization goal can be described as

$$\mathbf{\Lambda}\mathbf{g}_\text{ls} \approx \mathbf{0}. \tag{13}$$

The second optimization goal is to try to fulfill the Nyquist property and to minimize of the tail of the matched filter, simultaneously. Since $\mathbf{g}_\text{s}$ is the downsampled version of $\mathbf{g}$, the Nyquist property for $\mathbf{g}_\text{s}$ is obtained by placing $M = 2$ in (6). As a result, defining the matched filter as $\mathbf{p}_\text{s}$, the right half of $\mathbf{p}_\text{s}$ has the following properties

$$[\bar{\mathbf{p}}_\text{s}]_{n,1} = \mathbf{g}_\text{ls}^T\bar{\mathbf{S}}_n\mathbf{g}_\text{ls} = \begin{cases} 1, & n = 0 \\ 0, & n = 2\bar{n} \\ \text{arbitrary}, & n \neq 2\bar{n} \end{cases} \tag{14}$$

where $\bar{\mathbf{S}}_n = \mathbf{O}^\text{T}\mathbf{S}_n\mathbf{O}$, and $\mathbf{S}_n$ is a shift matrix so that $[\mathbf{S}_n]_{i,j} = \delta_{i,j+n}$ which performs shift-to-right for convolution. Defining $\mathbf{S} = [\bar{\mathbf{S}}_0; \bar{\mathbf{S}}_1; \ldots; \bar{\mathbf{S}}_{L_{g_\text{s}}}]$, the soft equality for $\bar{\mathbf{p}}_s$ can be written as

$$\bar{\mathbf{p}}_s = (\mathbf{I}_{L_{g_\text{s}}} \otimes \mathbf{g}_\text{ls})^\text{T}\mathbf{S}\mathbf{g}_\text{ls} \approx \boldsymbol{\delta}, \tag{15}$$

where $\boldsymbol{\delta} \in \mathbb{R}^{L_{g_\text{s}}\times 1}$ is an impulse vector, i.e. $[\boldsymbol{\delta}]_i = \delta_{i,1}$. In (15), we are seeking an ideal matched filter in which there is a unit sample at the centre of the filter, while its transient samples (tails) are minimized to zero.

Having the first and second soft equations (13) and (15), and defining $\mathbf{A} = [(\mathbf{I}_{L_{g_\text{s}}} \otimes \mathbf{g}_\text{ls})^\text{T}\mathbf{S}; \mathbf{\Lambda}]$ and $\mathbf{u} = [\boldsymbol{\delta}; \mathbf{0}]$, we can formulate the problem to find a solution for the unknown $\mathbf{g}_\text{ls}$, i.e.,

$$\mathbf{A}\mathbf{g}_\text{ls} \approx \mathbf{u}. \tag{16}$$

To solve (16), the error function is defined as

$$\xi = \|\mathbf{\Gamma}(\mathbf{A}\mathbf{g}_\text{ls} - \mathbf{u})\|^2, \tag{17}$$

where $\mathbf{\Gamma}$ is a diagonal matrix of weights to manage the emphasis on stopband and tail minimization, as well as the restriction on zero-crossings of the matched filter. This matrix is defined as

$$\mathbf{\Gamma} = \begin{bmatrix} \mathbf{\Theta} & \mathbf{0}_{L_{g_\text{s}}\times L_{g_\text{ls}}} \\ \mathbf{0}_{L_{g_\text{ls}}\times L_{g_\text{s}}} & \gamma\mathbf{I}_{L_{g_\text{ls}}} \end{bmatrix}, \tag{18}$$

where γ emphasizes the stopband attenuation, and $\mathbf{\Theta} \in \mathbb{R}^{L_{g_\text{s}}\times L_{g_\text{s}}}$ is formed as

$$[\mathbf{\Theta}]_{i,j} = \begin{cases} \beta, & i = j = 2\bar{n}+1, \bar{n} \geq 0 \\ \eta, & i = j = 2\bar{n}, \bar{n} \geq 3 \\ 0. & \text{otherwise} \end{cases} \tag{19}$$

In (19), β and η emphasize on zero-crossings and tail minimization, respectively. For β, η, and γ, zero value means *don't care*, while larger values result in more strict minimization.

Since $\mathbf{A}$ is a function of $\mathbf{g}_\text{ls}$, the error function in (17) is nonlinear with respect to $\mathbf{g}_\text{ls}$. Therefore, the optimum value for $\mathbf{g}_\text{ls}$ is found through an iterative process as in (20), in which

$$\mathbf{A}' = \begin{bmatrix} 2(\mathbf{I}_{L_{g_\text{s}}} \otimes \mathbf{g}_\text{ls})^\text{T}\mathbf{S} \\ \mathbf{\Lambda} \end{bmatrix}. \tag{21}$$

Proof of (20) and (21) is provided in the Appendix. The initial value $\mathbf{g}_\text{ls}^0$ in (20) can be a square-root raised cosine filter with roll-off factor α and arbitrary windowing. After sufficient iterations, $\mathbf{g}_\text{s}$ can be derived from the resulted $\mathbf{g}_\text{ls}$. For almost all the cases, the optimization converges to a solution within 10 iterations.

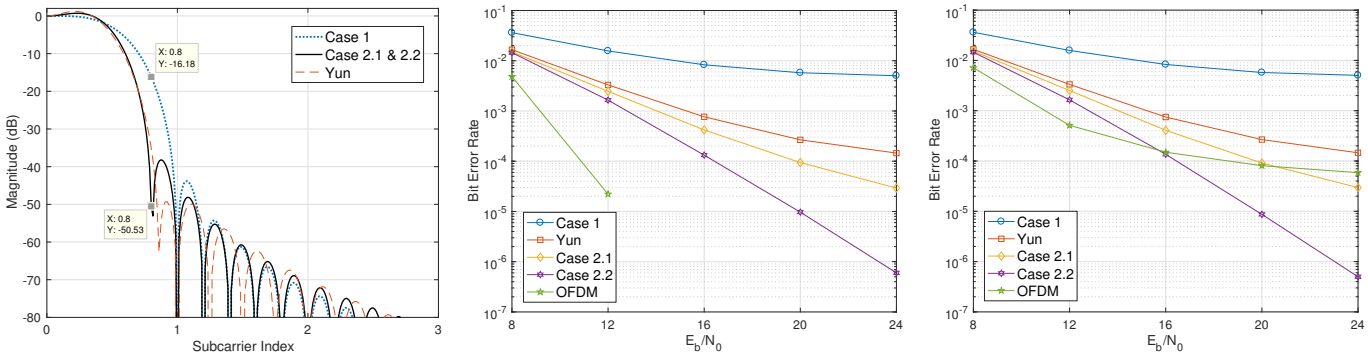

(a) (b) (c)

Fig. 2. Performance comparison of FBMC/QAM with the proposed filters vs. OFDM : a) PSD of the proposed filters in frequency domain, b) Synchronous performance, c) Asynchronous performance

B. Multicarrier Filter Discussions

The vector $\mathbf{g}_s$ is zero-padded at the sides to reach the size $2K$ and extract $\mathbf{G}_s$. In this design, we try to find β, η, and γ so that $G(K-1)$ and $G(-K+1)$ are approximately zero as shown in Fig. 1.(b). Using this approach, two of the dominant contributors to form $\mathbf{a}_n^{\text{ICI}}$ are minimized to zero, resulting in reduced energy of ICI. To do so, we release the strict Nyquist property by reducing β. Then, the residual ISI is compensated by choosing a proper ΔM for using in (7). It is worth mentioning that there is no straightforward way to calculate the parameters β, η, and γ according to the design goal. Thus, the best solution is to do exhaustive search of the parameters to get the desired filter characteristics.

IV. Simulation Results

In this section, we demonstrate the effectiveness of the proposed filter design. Similar to typical FBMC filters, we choose $L_{g_s} = 7$ for the designed filters. Also, $K = 5$ is chosen for the designs to provide enough room for the matched filter to fit within the FFT window. The filter coefficients are scaled so that the correct constellation is received. The modulation type for transmission is QPSK and the number of subcarriers is $M = 512$. The orthogonality provided by the filters are evaluated via signal to interference ratio (SIR) defined as $\|\mathbf{a}\|^2/\|\mathbf{a}-\hat{\mathbf{a}}\|^2$. Moreover, ΔM chosen for the filters is according to their zero-crossings in the time domain. If a filter satisfies the Nyquist property, then we choose $\Delta M = 0$. The results are also compared with Yun filter with $K = 4$ in [9]. Comparison of power spectral density (PSD) of the filters is provided in Fig. 2a. Bit error rate (BER) performance for synchronous and asynchronous uplink scenarios in the presence of added white Gaussian noise (AWGN) has been provided in Fig. 2b and 2c, respectively. In these scenarios, three adjacent subbands are used for data transmission and the performance of the middle subband is evaluated. In the synchronous scenario, there is no synchronization error between the subbands. While in the asynchronous scenario, there are random timing and carrier frequency offset between the subbands.

We discuss two scenarios using the proposed scheme. In the first scenario, a filter similar to conventional FBMC/OQAM systems has been designed. These filters are based on raised cosine filter with $\alpha = 1$. The specification is shown as case 1 in Table I. With emphasis on β, and less emphasis on η, and γ, this filter in quite close to the defined one as $\mathbf{g}_{\text{ls}}^0$. One can see that this filter has the lowest SIR among the filters, in which intrinsic interference mostly appears as ICI. This can be seen in Fig. 2a where case 1 is decaying slowly within the subcarrier spacing. Moreover, Fig. 2b shows the worst BER performance for this case.

TABLE I
Comparison of Filter Parameters and Results

	α	β	η	γ	ΔM	SEI	SIR(dB)
Case 1	0.99	5	0	1	0	100%	8.8
Case 2.1	0.3	1.58	11.62	1.97	0	100%	10.5
Case 2.2	0.3	1.58	11.62	1.97	37	93%	11
Yun [9]	-	-	-	-	0	100%	10.4

The second scenario is the optimized filter in frequency domain with less emphasis on the Nyquist property to minimize $G(K-1)$ and $G(-K+1)$. As shown in Fig. 2a, the corresponding point of $G(K-1)$, i.e. $(K-1)/K = 0.8$ shows approximately 35 dB improvement compared to case 1. This localization in the frequency domain comes with the cost of a little deviation from the Nyquist property in the time domain which is compensated by choosing a proper value for ΔM. To show the impact of ISI compensation, this scenario has been divided in to two cases 2.1 and 2.2. In the case 2.1, where $\Delta M = 0$, the SIR is as good as Yun filter as shown in Table I. By choosing $\Delta M = 37$ in the case 2.2, the SIR of the filter shows a significant enhancement and outperforms the rest of the filters. It is in fact a trade off between orthogonality and spectral efficiency.

Fig. 2b shows the BER performance in synchronous scenario. While both cases 2.1 and 2.2 show the superior performance compared to the others, it is quite clear that the ISI compensation in case 2.2 makes a remarkable enhancement in the performance of the system. These performances have also been compared with OFDM which shows that this orthogonal system has a considerably better performance when there are no synchronization errors. However, Fig. 2c shows that

OFDM incurs a significant performance degradation compared to FBMC systems in the asynchronous scenario. While the performance degradation of FBMC systems is negligible, OFDM performance reaches an error floor at higher SNRs. At lower SNRs, the residual intrinsic interference error is still dominant in FBMC which can be improved through the filter design.

Compared to the conventional and the state of the art FBMC filters, the performance of case 2.2 demonstrates its promising potential to be employed in FBMC systems.

V. Conclusion

In this paper, we investigated the filter design for FBMC/QAM systems. The system model of FBMC/QAM was derived with ability to compensate the ISI error, when the designed filter does not precisely provide the Nyquist property. Then, through the filter optimization problem, the stopband were minimized at the frequency sampling points to reduce the ICI energy between the adjacent subcarriers. The results showed significant enhancement in orthogonality provided by the optimized filter, compared to FBMC/OQAM filters and state of the art.

Acknowledgement

The authors would like to acknowledge the support of the University of Surrey 5GIC (http://www.surrey.ac.uk/5gic) members for this work.

Appendix
Proof of Nonlinear Problem Solving

We tackle the optimization problem by rewriting the error function in (17) as

$$\xi(\mathbf{g}_{\text{ls}}) = \big(\mathbf{\Gamma}(\mathbf{A}\mathbf{g}_{\text{ls}} - \mathbf{u})\big)^{\text{T}}\big(\mathbf{\Gamma}(\mathbf{A}\mathbf{g}_{\text{ls}} - \mathbf{u})\big). \tag{22}$$

Defining

$$\begin{aligned} \mathbf{w}(\mathbf{g}_{\text{ls}}) &= \mathbf{\Gamma}\mathbf{A}\mathbf{g}_{\text{ls}} \\ \bar{\mathbf{u}} &= \mathbf{\Gamma}\mathbf{u}, \end{aligned} \tag{23}$$

we can write the necessary condition to minimize $\xi(\mathbf{g}_{\text{ls}})$ through differentiation as [15]

$$\boldsymbol{\xi}'(\mathbf{g}_{\text{ls}}) = \mathbf{w}'(\mathbf{g}_{\text{ls}})\big(\bar{\mathbf{u}} - \mathbf{w}(\mathbf{g}_{\text{ls}})\big) = \mathbf{0}, \tag{24}$$

where $\mathbf{w}'(\mathbf{g}_{\text{ls}}) \in \mathbb{R}^{L_{g_{\text{ls}}} \times (L_{g_{\text{s}}} + L_{g_{\text{ls}}})}$ is the Jacobian matrix which with some manipulation can be derived as

$$\mathbf{w}'(\mathbf{g}_{\text{ls}}) = \frac{\partial \mathbf{w}(\mathbf{g}_{\text{ls}})^{\text{T}}}{\partial \mathbf{g}_{\text{ls}}} = \mathbf{\Gamma}\begin{bmatrix} 2(\mathbf{I}_{L_{g_{\text{ls}}}} \otimes \mathbf{g}_{\text{ls}})^{\text{T}}\mathbf{S} \\ \mathbf{\Lambda} \end{bmatrix} = \mathbf{\Gamma}\mathbf{A}'. \tag{25}$$

(24) is a set of $L_{g_{\text{ls}}}$ simultaneous nonlinear equations. They may be solved using the Newton-Raphson iteration method as

$$\mathbf{g}_{\text{ls}}^{k+1} = \mathbf{g}_{\text{ls}}^{k} - \Big(\frac{\partial \boldsymbol{\xi}'(\mathbf{g}_{\text{ls}})}{\partial \mathbf{g}_{\text{ls}}}\Big)^{-1}\boldsymbol{\xi}'(\mathbf{g}_{\text{ls}})\Big|_{\mathbf{g}_{\text{ls}}=\mathbf{g}_{\text{ls}}^{k}}. \tag{26}$$

The Jacobian of $\boldsymbol{\xi}'(\mathbf{g}_{\text{ls}})$ in (26), which is actually the scaled Hessian of $\xi(\mathbf{g}_{\text{ls}})$ is calculated as

$$\frac{\partial \boldsymbol{\xi}'(\mathbf{g}_{\text{ls}})}{\partial \mathbf{g}_{\text{ls}}} = \sum_{n=0}^{L_{g_{\text{s}}}+L_{g_{\text{ls}}}-1} \mathbf{w}_n''([\bar{\mathbf{u}}]_n - [\mathbf{w}]_n) - \mathbf{w}'^{\text{T}}\mathbf{w}', \tag{27}$$

in which

$$[\mathbf{w}_n'']_{i,j} = \frac{\partial^2[\mathbf{w}]_n}{\partial[\mathbf{g}_{\text{ls}}]_i \partial[\mathbf{g}_{\text{ls}}]_j} = \begin{cases} 2[\mathbf{\Gamma}]_{n,n}[\mathbf{S}_n]_{i,j}, & 0 \le n \le L_{g_{\text{s}}} - 1 \\ 0. & \text{otherwise} \end{cases} \tag{28}$$

Placing (28) in (27) results in

$$\frac{\partial \boldsymbol{\xi}'(\mathbf{g}_{\text{ls}})}{\partial \mathbf{g}_{\text{ls}}} = 2\sum_{n=0}^{L_{g_{\text{s}}}-1} [\mathbf{\Gamma}]_{n,n}\mathbf{S}_n([\bar{\mathbf{u}}]_n - [\mathbf{w}]_n) - \mathbf{w}'^{\text{T}}\mathbf{w}'. \tag{29}$$

Finally, by placing (29) and (23) in (26), (20) is achieved.

References

[1] L. Zhang, P. Xiao, A. Zafar, A. Quddus, and R. Tafazolli, "FBMC system: An insight analysis on double dispersive channel impact," *IEEE Transactions on Vehicular Technology*, vol. 66, no. 5, pp. 3942–3956, May 2017.

[2] Y. Yuan and X. Zhao, "5G: Vision, scenarios and enabling technologies," *ZTE Communications*, vol. 13, no. 1, pp. 3–10, March 2015.

[3] S. Taheri, M. Ghoraishi, P. Xiao, and L. Zhang, "Efficient implementation of filter bank multicarrier systems using circular fast convolution," *IEEE Access*, vol. 5, pp. 2855–2869, 2017.

[4] S. Taheri, M. Ghoraishi, P. Xiao, A. Cao, and Y. Gao, "Evaluation of preamble based channel estimation for MIMO-FBMC systems," *ZTE Communications*, vol. 14, no. 4, pp. 3–10, Oct 2016.

[5] R. Zakaria and D. Le Ruyet, "On spatial data multiplexing over coded filter-bank multicarrier with ML detection," *Personal Indoor and Mobile Radio Communications (PIMRC), 2011 IEEE 22nd International Symposium on*, pp. 1391–1395, Sept 2011.

[6] C. Lélé, P. Siohan, and R. Legouable, "The Alamouti scheme with CDMA-OFDM/OQAM," *EURASIP J. Adv. Signal Process*, vol. 2010, pp. 2:1–2:11, Jan. 2010.

[7] H. Nam, M. Choi, C. Kim, D. Hong, and S. Choi, "A new filter-bank multicarrier system for QAM signal transmission and reception," *2014 IEEE International Conference on Communications (ICC)*, pp. 5227–5232, June 2014.

[8] H. Nam, M. Choi, S. Han, C. Kim, S. Choi, and D. Hong, "A new filter-bank multicarrier system with two prototype filters for QAM symbols transmission and reception," *IEEE Transactions on Wireless Communications*, vol. 15, no. 9, pp. 5998–6009, Sept 2016.

[9] Y. H. Yun, C. Kim, K. Kim, Z. Ho, B. Lee, and J. Y. Seol, "A new waveform enabling enhanced QAM-FBMC systems," *2015 IEEE 16th International Workshop on Signal Processing Advances in Wireless Communications (SPAWC)*, pp. 116–120, June 2015.

[10] C. Kim, K. Kim, Y. H. Yun, Z. Ho, B. Lee, and J. Y. Seol, "QAM-FBMC: A new multi-carrier system for post-OFDM wireless communications," *2015 IEEE Global Communications Conference (GLOBECOM)*, pp. 1–6, Dec 2015.

[11] R. Zakaria and D. Le Ruyet, "On maximum likelihood MIMO detection in QAM-FBMC systems," *Personal Indoor and Mobile Radio Communications (PIMRC), 2010 IEEE 21st International Symposium on*, pp. 183–187, Sept 2010.

[12] R. Zakaria and D. L. Ruyet, "Intrinsic interference reduction in a filter bank-based multicarrier using QAM modulation," *Physical Communication*, vol. 11, no. Supplement C, pp. 15 – 24, 2014, radio Access Beyond OFDM(A).

[13] X. Yu, Y. Guanghui, Y. Xiao, Y. Zhen, X. Jun, and G. Bo, "FB-OFDM: A novel multicarrier scheme for 5G," *2016 European Conference on Networks and Communications (EuCNC)*, pp. 271–276, June 2016.

[14] B. Farhang-Boroujeny, "A square-root nyquist (M) filter design for digital communication systems," *IEEE Transactions on Signal Processing*, vol. 56, no. 5, pp. 2127–2132, May 2008.

[15] S. M. Kay, *Fundamentals of Statistical Signal Processing: Estimation Theory*. Upper Saddle River, NJ, USA: Prentice-Hall, Inc., 1993.